

Shear and magnification angular power spectra and higher-order moments from weak gravitational lensing

Andrew J. Barber^{1*} and A. N. Taylor²

¹*Astronomy Centre, University of Sussex, Falmer, Brighton, BN1 9QJ, U.K.*

²*Institute for Astronomy, University of Edinburgh, Royal Observatory, Blackford Hill, Edinburgh, U.K.*

Accepted 2001 —. Received 2001 —; in original form 2001 —

ABSTRACT

We present new results on the gravitational lensing shear and magnification power spectra obtained from numerical simulations of a flat cosmology with a cosmological constant. These results are of considerable interest since both the shear and the magnification are observables. We find that the power spectrum in the convergence behaves as expected, but the magnification develops a shot-noise spectrum due to the effects of discrete, massive clusters and symptomatic of moderate lensing beyond the weak-lensing regime. We find that this behaviour can be suppressed by “clipping” of the largest projected clusters. Our results are compared with predictions from a Halo Model-inspired functional fit for the non-linear evolution of the matter field and show excellent agreement. We also study the higher-order moments of the convergence field and find a new scaling relationship with redshift. In particular, the statistic S_3 is found to vary as $z_s^{-2.00 \pm 0.08}$ (where z_s is the source redshift) for the cosmology studied, which makes corrections for different median redshifts in different observational surveys particularly simple to apply.

Key words: Galaxies: clustering — Cosmology: gravitational lensing — Methods: numerical — Large-scale structure of Universe

1 INTRODUCTION

Knowing the distribution and evolution of the large-scale structure in the universe, together with the cosmological parameters which describe it, are fundamental to obtaining a detailed understanding of the cosmology in which we live. Studies of the effects of weak gravitational lensing in the images of distant galaxies are extremely useful in providing this information. In particular, since the gravitational deflections of light arise from variations in the gravitational potential along the light path, the deflections result from the underlying distribution of mass, usually considered to be in the form of dark matter. The lensing signal therefore contains information about the clustering of mass along the line-of-sight, rather than the clustering inferred from galaxy surveys which trace the luminous matter.

Most obviously, weak lensing induces a correlated distortion of galaxy images. The magnitude of the correlations depends on the density parameter, Ω_m , and the value of the vacuum energy density parameter, Ω_V , for the universe, as these parameters reflect both the amount of mass and the rate of evolution of structure. Consequently, the correlations

depend strongly on the redshifts of the lensed sources, as described by Jain & Seljak (1997) and Barber (2002). Recently a number of observational results have been reported for the so-called cosmic shear signal, which measures the variances in the shear on different angular scales. Bacon, Refregier & Ellis (2000), Kaiser, Wilson & Luppino (2000), Maoli et al. (2001), Van Waerbeke et al. (2000a, b), Wittman et al. (2000), Mellier et al. (2001), Rhodes, Refregier & Groth (2001), Van Waerbeke et al. (2001), Brown et al. (2002b), Bacon et al. (2002), Hoekstra, Yee & Gladders (2002), Hoekstra, Yee, Gladders, Barrientos, Hall & Infante (2002) and Jarvis et al. (2002) have all measured the cosmic shear and found good agreement with theoretical predictions.

In addition to shearing, weak gravitational lensing may cause a source at high redshift to become magnified or demagnified as a result of the amount and distribution of matter contained within the beam. The degree of magnification is strongly related to the convergence, which represents a projection of the density contrast, $\delta(x)$, at position x along the line of sight, and which is proportional to Ω_m . Consequently, measurements of statistics for the convergence are able to provide cosmological constraints, and comparisons of the power spectrum of the convergence with theoretical predictions and numerical values serve to validate our the-

* Email: A.J.Barber@sussex.ac.uk

oretical and numerical models (see, e.g., Moessner & Jain, 1998, and Jain, 2002).

Of particular importance for interpreting weak lensing statistics is the fact that the scales of interest lie largely in the non-linear regime (see, e.g., Jain, Seljak & White, 2000). On these scales, the non-linear gravitational evolution introduces non-Gaussianity to the convergence distribution, and this signature becomes apparent in higher-order moments, such as the skewness. In addition, the magnitude of the skewness values is very sensitive to the cosmology, so that measurements of higher-order statistics in the convergence may be used as discriminators of cosmology.

In this work, we have obtained weak lensing statistics from cosmological N -body simulations using an algorithm described by Couchman, Barber & Thomas (1999) which computes the three-dimensional shear in the simulations. The code has been applied to cosmological simulations with $\Omega_m = 0.3$ and $\Omega_V = 0.7$; cosmologies of this type will be referred to as LCDM cosmologies. To obtain the required statistics on different angular scales, the computed shear values have been combined (using the appropriate angular diameter distance factors and accounting for multiple deflections) along lines of sight arranged radially from the observer's position at redshift $z = 0$. Detailed results are presented for background sources at 14 different redshifts ($z_s = 0.1$ to 3.6) and angular scales from $1'$ to $32'$.

As a test of the accuracy of non-linear fits to the convergence power we compare the numerically generated convergence power spectra with our own theoretically predicted convergence spectra based on a Halo Model fit to numerical simulations (Smith et al., 2002). We also investigate the statistical properties of the magnification power spectrum and test predictions of the weak lensing regime. We also report on the expected redshift and scale dependence for higher-order statistics in the convergence.

A brief outline of this paper is as follows. In Section 2, we define the shear, reduced shear, convergence and magnification in weak gravitational lensing and outline how the magnification and convergence values are obtained in practice from observational data. In Section 3 we describe the relationships between the power spectra for the convergence, shear and magnification fluctuations, and how the power spectrum for the convergence relates to the matter power spectrum. We also describe our methods for computing the convergence power in the non-linear regime. Also in this Section, the higher-order moments of the non-linear convergence field are defined. The numerical procedure we use to generate the shear, convergence and magnification fields from the simulations are presented in Section 4, while in Section 5 we present our results for the numerical and theoretical comparison of the convergence power spectra, the power in the magnification fluctuations, and the higher-order moments, particularly the S_3 statistic. Finally we discuss the results and present our conclusions in Section 6.

2 WEAK LENSING FIELDS

2.1 Weak shear

Ellipticity measurements of observed galaxy images can be used to estimate the lensing shear signal. One definition for

the ellipticity (see, e.g., Blandford et al., 1991, and Bartelmann & Schneider, 2001) is the complex ellipticity,

$$\epsilon = \frac{Q_{11} - Q_{22} + 2iQ_{12}}{Q_{11} + Q_{22} + 2(Q_{11}Q_{22} - Q_{12}^2)^{\frac{1}{2}}}, \quad (1)$$

in which Q_{ij} is the tensor of second brightness moments for a fixed isophotal contour.

The “reduced shear,” g , for a galaxy image at angular position θ , is defined by

$$g(\theta) \equiv \frac{\gamma(\theta)}{1 - \kappa(\theta)}, \quad (2)$$

where γ is the complex shear and κ is the lensing convergence. Both γ and κ are obtained as projections from the values of the second derivatives of the lensing potential along the light path. Their detailed definitions and their relationships to the lensing potential are given by Schneider, Ehlers & Falco (1992) and summarised by Barber (2002). The transformation between the source ellipticities, $\epsilon^{(s)}$, and the image ellipticities, ϵ , is given by

$$\epsilon^{(s)} = \frac{\epsilon - g}{1 - g^* \epsilon} \quad (3)$$

for $|g| \leq 1$. The asterisk in equation (3) denotes the complex conjugate. In the case of weak lensing, for which κ , $|\gamma|$ and $|g|$ are much less than unity, the transformation reduces to

$$\epsilon \simeq \epsilon^{(s)} + g \quad (4)$$

for low intrinsic source ellipticities.

The intrinsic ellipticities of given galaxies are not known, but averaging over the binned galaxy distribution, and assuming random ellipticities, yields a net lens shear:

$$\gamma \simeq g \simeq \langle \epsilon \rangle. \quad (5)$$

This equality suggests that for weak lensing the variances in both the shear and the reduced shear for a given angular scale are expected to be similar. However, from numerical simulations, Barber (2002) has given explicit expressions for both as functions of redshift and angular scale, which show the expected differences.

It is also possible to reconstruct the convergence from the shape information alone, up to an arbitrary constant, using methods such as those described by Kaiser & Squires (1993) and Seitz & Schneider (1996) for the two-dimensional reconstruction of cluster masses. Kaiser (1995) generalised the method for applications beyond the linear regime.

Drawbacks to the reconstruction method arise from contamination by intrinsic galaxy alignments (Pen, Lee & Seljak, 2000, Brown et al., 2002a, Crittenden et al., 2001, Cate-lan, Kamionkowski & Blandford, 2001, Mackey, White & Kamionkowski, 2002, Heavens, Refregier & Heymans, 2000, and Croft & Metzler, 2001), although these can be statistically removed if redshift information is available (Heyman & Heavens, 2002, and King & Schneider, 2002). In addition, map-making of the convergence field over a finite area suffers from non-local effects due to missing information beyond the survey area (Bacon & Taylor, 2002). For these reasons it is useful to have an alternative method for estimating the convergence.

2.2 The magnification effect

The lensing magnification, μ , can be computed directly from

$$\mu = (|\det \mathcal{A}|)^{-1} = \frac{1}{|(1 - \kappa)^2 - \gamma^2|}, \quad (6)$$

where \mathcal{A} is the two-dimensional Jacobian matrix which describes the mapping of a source onto its image. The effect of magnification on galaxy source counts results in a decrease due to the increase in the lensed image area, and an increase in counts due to the brightening of galaxies allowing their inclusion in a flux-limited catalogue. For a power-law flux distribution, the effect of lensing is (Broadhurst, Taylor & Peacock, 1995, and Bartelmann & Schneider, 2001):

$$n_0(> S, z) \simeq \mu(z)^{\alpha-1} n(> S, z), \quad (7)$$

where $n(> S, z)$ and $n_0(> S, z)$ are the lensed and unlensed number of galaxy images per unit solid angle with flux greater than S and with redshift within dz of z , and α is the power-law exponent of S . Hence with calibration of the underlying number count amplitude and slope it is possible to estimate the magnification averaged over redshift.

Alternatively, magnification values may be obtained from the change in image sizes at fixed surface brightness. This method is described in detail by Bartelmann and Narayan (1995) and summarised concisely by Bartelmann and Schneider (2001). See also Jain (2002) for a recent discussion.

Estimates of the lensing magnification based on number counts suffer from noise arising from the intrinsic clustering of the source galaxies, if redshift information is not available (e.g., Broadhurst, Taylor & Peacock, 1995, and Bartelmann & Schneider, 2001). With redshift information one should either select galaxies at different redshifts to remove the intrinsic clustering signal, or use the brightening effect behind structure (Dye et al., 2001). Size distortions may also be affected if size is correlated with the environment. Again this may be removed by selecting galaxies at different redshifts.

While the magnification signal-to-noise ratio is generally poorer than that of the shear reconstruction method, it is valuable as an independent signal. Furthermore, if good values for the convergence are available, then the higher-order statistics are potentially very fruitful in discriminating amongst cosmologies (see, e.g., Bernardeau, Van Waerbeke & Mellier, 1997, and Jain et al., 2000).

Finally, the convergence can be expressed (see Jain et al., 2000, for example) as a projection of the density contrast, $\delta(\boldsymbol{\theta}, x_3)$:

$$2\kappa(\boldsymbol{\theta}, x_s) = \frac{3H_0^2\Omega_m}{2c^2} \int_0^{x_s} dx_3 \frac{D(x_3)D(x_s - x_3)}{D(x_s)} \frac{\delta(\boldsymbol{\theta}, x_3)}{a(x_3)}, \quad (8)$$

where $\boldsymbol{\theta}$ is the direction angle of the source at distance x_s along the coordinate direction x_3 , H_0 is the Hubble parameter, $D(x_3)$, $D(x_s - x_3)$ and $D(x_s)$ are the angular diameter distances to position x_3 , x_s to x_3 , and to position x_s , respectively, and a is the scale factor.

Although the lens convergence depends on the distance to the source galaxy this dependence is usually lost by averaging over the source distribution. However with redshift information the full three-dimensional distribution of the density field can be fully recovered (Taylor, 2001, and Bacon & Taylor, 2002).

3 STATISTICAL PROPERTIES OF LENSING FIELDS

3.1 The power spectra

The convergence field can be expanded in two-dimensional Fourier modes on a flat-sky:

$$\kappa(\boldsymbol{\ell}) = \int d^2\theta \kappa(\boldsymbol{\theta}) e^{i\boldsymbol{\ell} \cdot \boldsymbol{\theta}}, \quad (9)$$

where $\boldsymbol{\ell}$ is the angular wavenumber. The two-point correlation of these modes defines the power spectrum, $C_\ell^{\kappa\kappa}$:

$$\langle \kappa(\boldsymbol{\ell}) \kappa^*(\boldsymbol{\ell}') \rangle = (2\pi)^2 C_\ell^{\kappa\kappa} \delta_D(\boldsymbol{\ell} - \boldsymbol{\ell}'). \quad (10)$$

Since the convergence can be expressed in the form of a projection of the density contrast, the power spectrum for the effective convergence can be obtained in terms of the matter power spectrum, $P_\delta(k)$, for the density contrast (e.g., Bartelmann & Schneider, 2001):

$$C_\ell^{\kappa\kappa} = \frac{9H_0^4\Omega_m^2}{4c^4} \int_0^{w_H} dw \left(\frac{\overline{W}(w)}{a(w)} \right)^2 P_\delta\left(\frac{\ell}{w}, w\right), \quad (11)$$

where the integral is evaluated over the comoving radial coordinate, w , from 0 to the horizon, w_H , defined by

$$w_H = c \int \frac{dz}{H(z)}, \quad (12)$$

where $H(z) = H_0[(1+z)^3\Omega_m + \Omega_V]^{1/2}$ and where we have assumed a spatially flat universe; the weighting function, \overline{W} , can be expressed as

$$\overline{W}(w) \equiv \int_w^{w_H} dw' G(w') \frac{w' - w}{w'}, \quad (13)$$

where $G(w)dw = p_z(z)dz$, where $p_z(z)$ is the matter distribution function.

On angular scales smaller than about $10'$, the total power in the effective convergence per logarithmic interval in wavenumber, $\ell(\ell+1)C_\ell^{\kappa\kappa}/(2\pi)$, is dominated by galaxy clusters. Jain et al. (2000) show that for the scales of interest in weak lensing, $\ell(\ell+1)C_\ell^{\kappa\kappa}/(2\pi)$ lies almost entirely in this regime, and there is significant enhancement (approximately an order of magnitude) of the power over linear predictions on scales below $\ell \simeq 10^4$.

The two-point statistical properties of the shear and convergence are closely related. In the flat sky approximation the components γ_1 and γ_2 of the shear are related to the effective convergence, κ , in Fourier space (e.g., Barber, 2002):

$$\tilde{\gamma}_1^2(\boldsymbol{\ell}) + \tilde{\gamma}_2^2(\boldsymbol{\ell}) = \tilde{\kappa}^2(\boldsymbol{\ell}). \quad (14)$$

Then it is clear that the power spectra for the shear, $C_\ell^{\gamma\gamma}$, and the convergence, $C_\ell^{\kappa\kappa}$, are the same in the case of weak lensing.

Finally, in the weak lensing regime, equation (6) reduces to

$$\mu = 1 + \delta\mu \simeq 1 + 2\kappa, \quad (15)$$

so that

$$C_\ell^{\delta\mu\delta\mu} \simeq 4C_\ell^{\kappa\kappa} = 4C_\ell^{\gamma\gamma}, \quad (16)$$

where $C_\ell^{\delta\mu\delta\mu}$ is the power in the magnification fluctuation, $\delta\mu$. This relation is questionable, since in general it is not

obvious that the weak lensing regime will hold over the whole magnification field. In particular, the denominator of the expression for μ in equation (6) is sensitive to the value of κ near peaks in the convergence field. We shall test this dependence in Section 5.2.

3.2 Non-linear evolution of the matter field

So long as the gravitational potential field is small the perturbations in the matter density field can be fully non-linear. The three-dimensional gravitational potential, $\Phi(\mathbf{x})$, is related to arbitrary perturbations in the mass-density field by Poisson's equation,

$$(\nabla^2 + 3H_0^2\Omega_K)\Phi(\mathbf{x}) = -\frac{3}{2}H_0^2\Omega_m(1+z)\delta(\mathbf{x}, z), \quad (17)$$

where Ω_K is the curvature energy-density parameter.

A number of useful techniques have emerged to allow us to transform from the linear matter power spectrum to a fully non-linear spectrum. The first of these originated from the work of Hamilton et al. (1991) who considered the evolution of the matter correlation function, and was extended by Peacock & Dodds (1996) to account for the non-linear evolution of the matter power spectrum. These methods are based on the conservation of mass and a rescaling of physical lengths due to gravitational collapse. These fits generally are accurate to around the 10% level.

More recently Peacock & Smith (2000) and Seljak (2000) have developed a model for the non-linear evolution of the power spectrum based on the random distribution of dark matter haloes, modulated by the large-scale matter distribution. This Halo Model for non-linear evolution reproduces the matter power spectrum of N -body simulations over a wide range of scales and has the advantage of relating the linear and non-linear power at the same scale. Given the utility of the non-linear fitting formula, Smith et al. (2002) have presented a new set of fitting functions based on the Halo Model functional form and calibrated to a set of N -body simulations. These prove to be far more accurate ($\sim 1\%$) than previous formulæ. However these fits are only as accurate as the underlying simulations used in the fitting, which in this case were provided by the VIRGO Consortium[†]. In this paper we shall use the latter, more accurate fits based on the Halo Model functional form. While Smith et al. (2002) have compared their fit to the non-linear matter power spectrum, here we compare for the first time the predicted convergence power with the results of our simulations in Section 5.1.

3.3 Higher-order moments in the convergence

In addition to two-point statistics, higher-order statistical properties of the lensing fields are also of interest as non-linear evolution of the density field will introduce non-Gaussianity (e.g., Jain et al., 2000). Bernardeau et al. (1997) have investigated analytically the dependence of higher-order moments in the convergence on the cosmological parameters, and in particular have discussed the ratio

$$S_3(\theta) \equiv \frac{\langle \kappa^3(\theta) \rangle}{\langle \kappa^2(\theta) \rangle^2}. \quad (18)$$

The significance of the S_3 statistic is that it is expected to be independent of the normalisation of the power spectrum, and can also be shown to be rather insensitive to the angular scale.

In the case of $\Omega_V = 0$, Bernardeau et al. (1997) have shown that

$$S_3(\Omega_m) \simeq -42\Omega_m^{-0.8} \quad (19)$$

for $z_s \simeq 1$. The Ω_m dependence is slightly weaker for sources at high redshift, and at low redshift S_3 becomes approximately inversely proportional to Ω_m . The redshift dependence of S_3 in an Einstein-de Sitter cosmology is approximately $z_s^{-1.35}$.

Jain et al. (2000) have investigated the values for S_3 in different cosmologies for sources at $z_s = 1$, including an LCDM cosmology using N -body simulations based on reconstructing the convergence values from the shear, and including the effects of noisy data. Using various statistics based on the reconstructed convergence, they show that there are clear differences in the S_3 values between the LCDM cosmology and an open cosmology, and also claim that Ω_m can be constrained to within an uncertainty of 0.1 – 0.2 in a deep survey of several square degrees. We shall study the S_3 statistic in more detail in Section 5.3.

4 NUMERICAL PROCEDURE

To evaluate the weak lensing statistics, we have applied the algorithm for computing the shear in three dimensions, as described by Couchman et al. (1999) to the cosmological N -body simulations of the Hydra Consortium[‡] produced using the ‘Hydra’ N -body hydrodynamics code (Couchman, Thomas & Pearce, 1995). Simulations of the LCDM Dark Matter only cosmology were used with $\Omega_m = 0.3$, $\Omega_V = 0.7$, power spectrum shape parameter $\Gamma = 0.25$ and normalisation, σ_8 , on scales of $8h^{-1}\text{Mpc}$ of 1.22. The number of particles, each of mass $1.29 \times 10^{11}h^{-1}$ solar masses, was 86^3 and the minimum value of the (variable) particle softening was chosen to be $0.0007(1+z)$ in box units. The simulation volumes had comoving side dimensions of $100h^{-1}\text{Mpc}$. To avoid obvious structure correlations between adjacent boxes, each was arbitrarily translated, rotated (by multiples of 90°) and reflected about each coordinate axis, and in addition, each complete run was performed 10 times.

The general procedure for establishing the locations within the simulations for the computations of the shear and for computing the values of the elements of the shear matrices, is as described by Barber (2002), with the multiple lens plane theory being applied along the lines of sight. In this work, a total of 455×455 lines of sight were used and 300 evaluation locations for the three-dimensional shear along each line of sight in each simulation volume, thereby allowing regular sampling of the $2.6^\circ \times 2.6^\circ$ field of view. With this number of lines of sight, the angular resolution equates to the minimum value of the particle softening at the optimum redshift, $z = 0.36$, for lensing of sources at

[†] <http://star-www.dur.ac.uk/~frazierp/virgo/virgo.html>

[‡] (<http://hydra.mcmaster.ca/hydra/index.html>)

a redshift of 1. To allow for the larger angular size of the minimum softening at low redshifts and also for the range of particle softening scales above the minimum value, a resolution limit of 1 arcminute has been adopted for the data analyses.

A total of 14 source redshift slices were selected to give good statistical coverage of the redshifts of interest. These were redshifts of $z_s = 0.10, 0.21, 0.29, 0.41, 0.49, 0.58, 0.72, 0.82, 0.88, 0.99, 1.53, 1.97, 3.07$ and 3.57 , corresponding to the redshifts of the simulation boxes. Hereafter, we shall only quote these redshifts to one decimal place for brevity.

From the statistics computed in each of the 10 simulation runs, we computed the variances, the skewnesses, the statistic S_3 , and the power spectra for each of the source redshifts. The two-point and higher-order moments were computed on angular scales of $1'.0, 2'.0, 4'.0, 8'.0, 16'.0$ and $32'.0$ using a top-hat filter, and the power spectra values were computed for a set of 15 wavenumber bins, spaced logarithmically. Here we report on the results for these statistics as computed for the effective convergence and the magnification fluctuation (i.e., the departure of the magnification value from unity). We computed these statistics from the convergence values directly, rather than on convergence values reconstructed from the shear.

For the power spectra, the square of the absolute values of the Fourier transform of the convergence or magnification fluctuation were normalised by multiplication by $\frac{L^2}{(2\pi)^2} \cdot 2\pi\ell^2$, where L is the angular length of the map side in radians. With this definition of the power spectrum, the results are essentially equivalent to $\ell(\ell+1)C_\ell^{\kappa\kappa}/(2\pi)$.

The computed values for the required statistics from each of the $N = 10$ runs were averaged, and the errors on the means of $1\sigma/\sqrt{N}$ determined. However, since we found the power in the magnification fluctuation to be a very noisy statistic, we have determined the median values and computed the errors on the medians for $C_\ell^{\delta\mu\delta\mu}/4$.

5 RESULTS

5.1 Comparison of the convergence power spectra with theoretical predictions.

We have verified from our simulation results the equivalence of the shear and convergence power spectra. The shear statistics, in particular the shear variance, and their redshift dependence are described fully in Barber (2002). Here we present our results for the convergence power spectra for sources at the different redshifts obtained from our weak lensing simulations and from the linear and non-linear theory predictions.

The convergence power spectra values from the weak lensing simulations are available for all the selected source redshifts. Figure 1 shows a comparison of the power spectra from our simulations with linear theory and the non-linear convergence power based on the Halo Model-inspired fitting functions of Smith et al. (2002) for sources at redshifts 0.5, 1.0 and 2.0. We see that our numerical results lie primarily in the non-linear regime and that there is good agreement between the non-linear predictions and our simulations. Notable discrepancies are apparent only for the highest redshifts and in the highly non-linear regime, where we expect

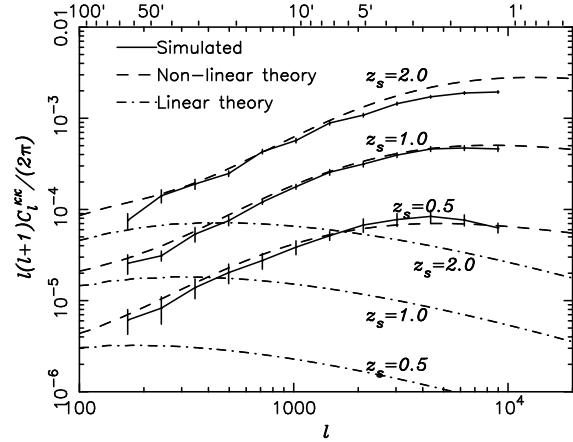


Figure 1. Simulated $\ell(\ell+1)C_\ell^{\kappa\kappa}/(2\pi)$ values (full lines) together with the linear (dot-dashed lines) and non-linear (dashed lines) predictions based on the Smith et al. (2002) Halo Model-inspired fitting formula, for $z_s = 0.5$ (lowest set of curves), 1.0 (middle set) and 2.0 (uppermost set).

the variance in the convergence field to be greatest. In terms of the simulation data for redshifts greater than 1, our field of view is effectively smaller because we make use of the periodicity in the simulations when lines of sight extend outside the volumes. Consequently, we sample in real terms a more limited area of sky, which suggests that the quoted error bars for the high redshift data may be understated. For the Halo-model, we simply note that its predictions may not adequately account for the presence of voids and detailed structure in the dark matter halos which become increasingly important in terms of their gravitational lensing effects for high redshift sources.

5.2 The power in the magnification fluctuations

We saw in Section 3.1 that the power in the magnification fluctuation, $C_\ell^{\delta\mu\delta\mu}$, is expected to be four times the shear and the convergence power. This result follows from making the assumption of weak lensing, where $\delta\mu \equiv \mu - 1$ is taken to be equal to 2κ . At low redshift, where the lensing may be considered to be weak on most scales, $C_\ell^{\delta\mu\delta\mu}/4$ and $C_\ell^{\kappa\kappa}$ are consistent with each other and with the weak lensing approximation. However, as the source redshift increases, we see increasing departures from this equality. Figures 2, 3, 4, 5 and 6 compare $\ell(\ell+1)C_\ell^{\delta\mu\delta\mu}/(8\pi)$ and $\ell(\ell+1)C_\ell^{\kappa\kappa}/(2\pi)$ for source redshifts of 0.5, 0.8, 1, 1.5 and 2 respectively. The departures are seen at first just on small scales (where the lensing is expected to be stronger), until, finally, at the highest redshifts, the departure is not only significant, but becomes consistent with a Poisson distribution for the magnification fluctuations on all scales. In support of this effect, we noticed the presence of large variations in the magnification power from one simulation run to the next for sources at high redshift. Because of these large variations, the curves have been plotted for the median power values in the magnification, rather than the mean, which would have been strongly influenced by the large power values.

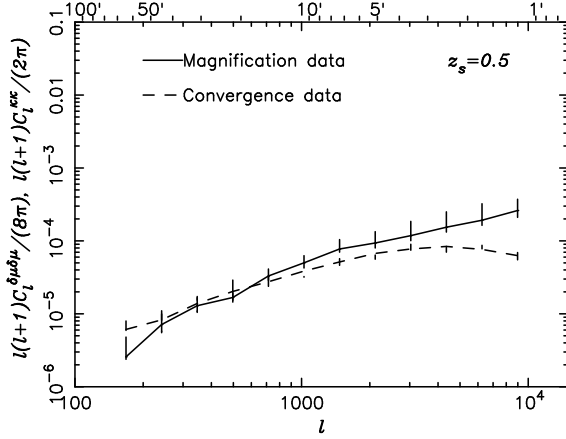


Figure 2. Median $\ell(\ell+1)C_\ell^{\delta\mu\delta\mu}/(8\pi)$ and mean $\ell(\ell+1)C_\ell^{\kappa\kappa}/(2\pi)$ for $z_s = 0.5$.

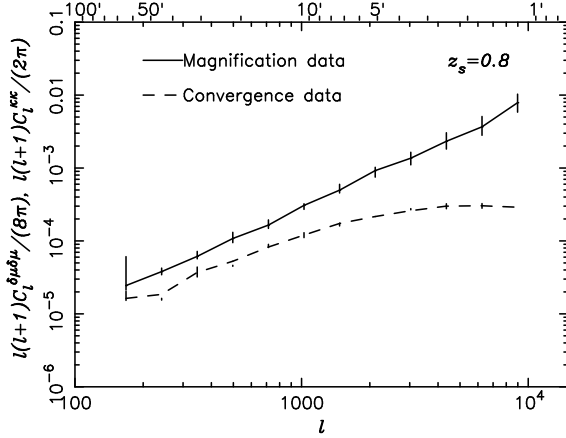


Figure 3. Median $\ell(\ell+1)C_\ell^{\delta\mu\delta\mu}/(8\pi)$ and mean $\ell(\ell+1)C_\ell^{\kappa\kappa}/(2\pi)$ for $z_s = 0.8$.

The departures in $C_\ell^{\delta\mu\delta\mu}/4$ from $C_\ell^{\kappa\kappa}$ arise from medium and strong lensing events. By making cuts in the data at the extreme ends, we are able to show the effects of high magnification events. Figure 7 reproduces the magnification and convergence data from Figure 4 and also shows $\ell(\ell+1)C_\ell^{\delta\mu\delta\mu}/(8\pi)$ and $\ell(\ell+1)C_\ell^{\kappa\kappa}/(2\pi)$ after making cuts in the data beyond 6σ and 1σ in their distributions. When the extreme magnification (and convergence) events are excluded, we see that the apparent Poisson distribution in the magnification is removed and the curve reverts to the more “normal” behaviour expected from lower redshift sources. Thus we can conclude that it is the very high magnifications which dominate the signal, although there is clear evidence of departures even for moderate levels of magnification. Our simulations have a relatively high value for the normalisation, σ_8 , when compared with very recent determinations (e.g., Brown et al., 2002b) and we might expect this to lead to a higher number of clusters than in cosmologies with a lower σ_8 . Consequently, the shot-noise effect we

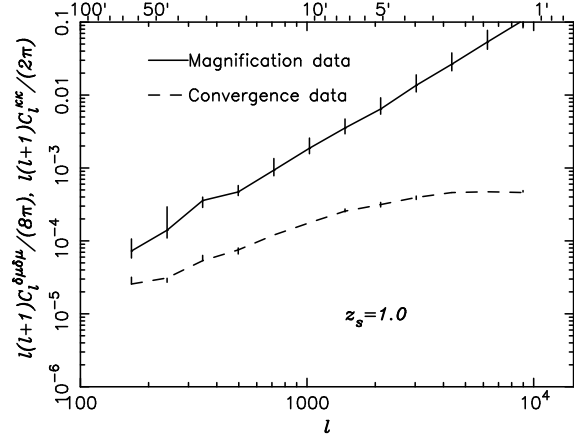


Figure 4. Median $\ell(\ell+1)C_\ell^{\delta\mu\delta\mu}/(8\pi)$ and mean $\ell(\ell+1)C_\ell^{\kappa\kappa}/(2\pi)$ for $z_s = 1$.

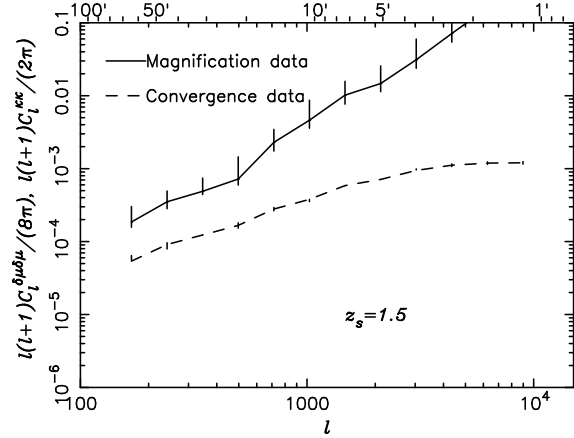


Figure 5. Median $\ell(\ell+1)C_\ell^{\delta\mu\delta\mu}/(8\pi)$ and mean $\ell(\ell+1)C_\ell^{\kappa\kappa}/(2\pi)$ for $z_s = 1.5$.

describe may be moderated, although still present, in a universe with a lower normalisation value.

5.3 Higher-order moments

In Figure 8 we plot the $S_3(\theta, z_s)$ statistic for the convergence, which is a known discriminator of cosmology and independent of the matter power spectrum normalisation, for four different source redshifts and for angular scales from $1'.0$ to $32'.0$.

The redshift variation of $S_3(\theta, z_s)$ for the different angular scales is displayed in Figure 9. On scales larger than $8'.0$ the errors in the measurements are greater, and these have not been plotted for clarity. By writing

$$S_3(\theta, z_s) \equiv a(\theta)z^{b(\theta)}, \quad (20)$$

with θ expressed in arcminutes, we find

$$a(\theta) = (116 \pm 6) - (7.4 \pm 1.9)\theta \quad (21)$$

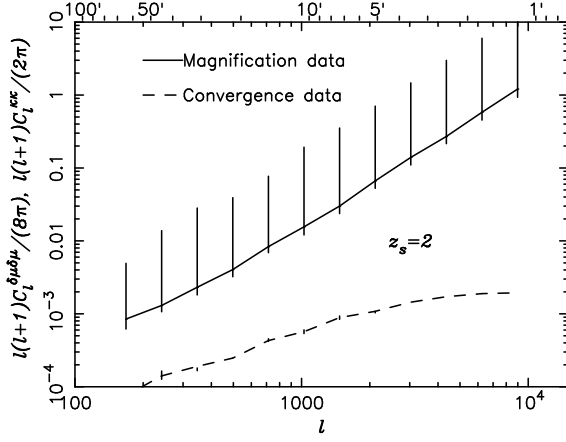


Figure 6. Median $\ell(\ell+1)C_{\ell}^{\delta\mu\delta\mu}/(8\pi)$ and mean $\ell(\ell+1)C_{\ell}^{\kappa\kappa}/(2\pi)$ for $z_s = 2$.

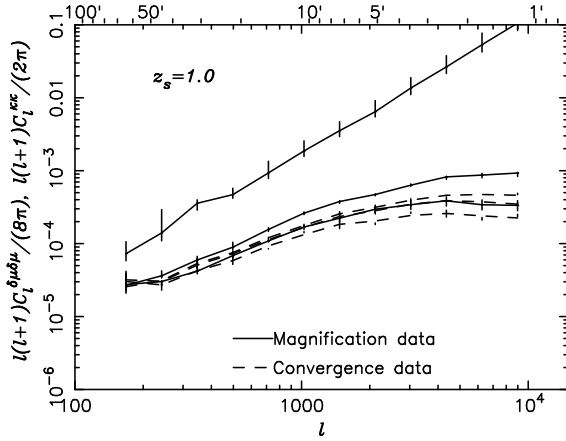


Figure 7. The three solid curves represent the median $\ell(\ell+1)C_{\ell}^{\delta\mu\delta\mu}/(8\pi)$ for the full magnification distribution (upper curve), and the cut distributions beyond 6σ (middle solid-line curve) and 1σ (lower solid-line curve) for $z_s = 1$. These are compared with the equivalent curves for the mean $\ell(\ell+1)C_{\ell}^{\kappa\kappa}/(2\pi)$ for the convergence (dotted-line curves).

and

$$b(\theta) = -(2.00 \pm 0.08), \quad (22)$$

i.e., b is independent of θ at a constant value, so that we may write, without the error values for clarity,

$$S_3(\theta, z_s) \simeq (116 - 7.4\theta)z_s^{-2.00} \quad (23)$$

for $1' \leq \theta \leq 8'$. The fitting to this formula is excellent for all source redshifts up to and including 1, appropriate to most recent galaxy surveys. The precise $z_s^{-2.00}$ dependence for S_3 is also particularly simple to apply when combining or making comparisons with different surveys in which the median redshifts for the galaxies may be different, making this relationship particularly valuable.

In Figure 10 we have determined the values of

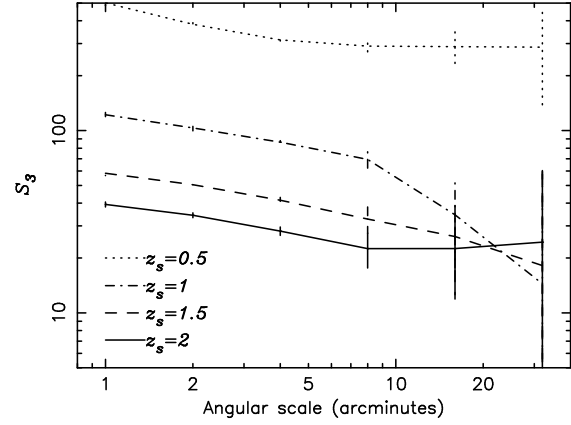


Figure 8. $S_3(\theta, z_s)$ vs. θ for $z_s = 0.5$ (dotted line), 1 (dashed-dotted line), 1.5 (dashed line) and 2 (solid line).

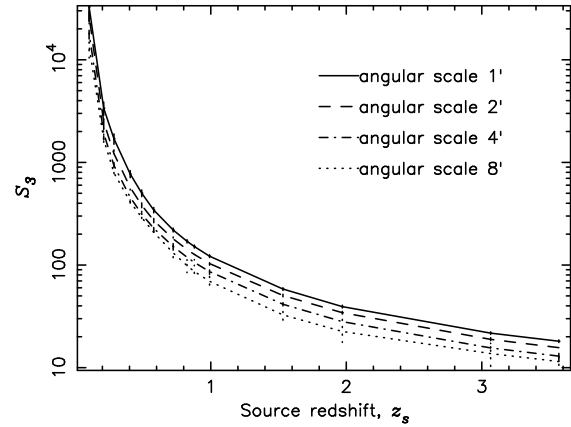


Figure 9. $S_3(\theta, z_s)$ vs. z_s at angular scales of $1'.0$, $2'.0$, $4'.0$ and $8'.0$.

$(S_3\sigma_{\kappa}^2)(\theta, z_s)$, where σ_{κ}^2 represents the variance in the convergence, for the different source redshifts. For a given angular scale, this product was found to be almost independent of redshift for an Einstein-de Sitter universe by Bernardeau et al. (1997) and we find a similar behaviour in the LCDM cosmology here, particularly at high redshift. Because of the independence from redshift, there is no need to adjust this statistic when making comparisons amongst different surveys, provided the median redshifts are not too small. This fact makes this statistic particularly useful for the discrimination of cosmologies.

Our results for $S_3\sigma_{\kappa}^2$ at low redshift are supported by combining the shear variance, $\sigma_{\gamma}^2 \equiv \langle \gamma^2(\theta, z_s) \rangle \approx \sigma_{\kappa}^2$, with the expression for $S_3(\theta, z_s)$ given by equation (23). Barber (2002) has shown that

$$\langle \gamma^2(\theta, z_s) \rangle = \langle \kappa^2(\theta, z_s) \rangle \propto z_s^{2.07 \pm 0.04}, \quad (24)$$

for source redshifts $z_s \leq 1.6$ and angular scales of $2'.0 \leq \theta \leq 32'.0$, so that the combination

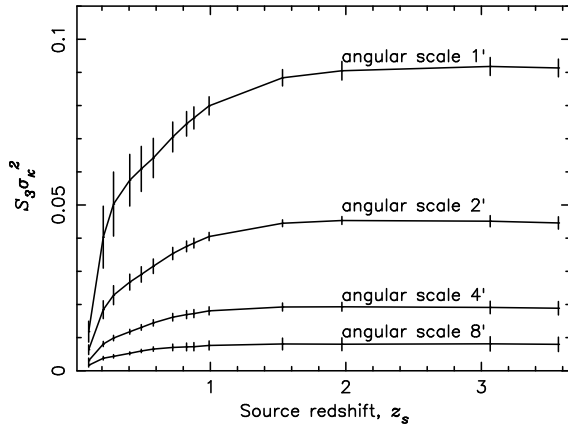


Figure 10. $S_3\sigma_\kappa^2$ vs. z_s for angular scales of $1'.0$, $2'.0$, $4'.0$ and $8'.0$.

$$S_3\sigma_\kappa^2(\theta, z_s) \propto z_s^{2.07 \pm 0.04} \cdot z_s^{-(2.00 \pm 0.08)} \quad (25)$$

predicts the very slowly rising function of redshift for $z_s < 1$ and $2'.0 \leq \theta \leq 8'.0$, which are the ranges of applicability common to both results.

6 DISCUSSION AND CONCLUSIONS

6.1 Discussion

We have shown that the convergence power spectrum values computed directly from the weak lensing simulations show remarkably good agreement with the non-linear predictions for the convergence power based on the Smith et al. (2002) Halo Model-inspired fitting formulæ. Whilst we have not compared the predictions for other cosmological models in this paper, the same numerical data, together with equivalent data for an open cosmology, have been compared with the predictions from Hierarchical models for the density field. Valageas, Barber & Munshi (2003) have shown excellent agreement for the full probability distribution functions for the shear and Barber, Munshi & Valageas (2003) have shown agreement with predictions for the convergence and higher-order moments. Consequently, these several agreements give us considerable confidence in our lensing procedure and the resulting weak lensing data, which we have here analysed in a number of ways.

Our results for the power in the magnification fluctuation suggest that the observed magnifications should be treated with some care as an estimate of the convergence power. This is especially true on small scales and at high redshift, since the magnification is very sensitive to locally high values of the convergence (arising from the tail of the skewed convergence distribution) and may vary significantly across small angular intervals. It further confirms that the weak lensing regime for the magnification should be treated with care, even for galaxy surveys with a mean redshift of 0.8. Worse, at a redshift of 1, where many surveys have been undertaken or planned, the magnification power may be extremely noisy. Consequently, evaluation of the convergence

from magnification measurements is clearly likely to be biased by isolated high peaks in the convergence and shear fields.

The origin of this effect is the appearance of a few regions of very high magnification in the simulations. The spectrum is dominated by the strongest magnification events, although the signal shows moderate departures from the expected values even for medium magnifications. Since in an LCDM universe clusters form earlier and have time to relax, we expect large clusters to generate a large shear field. It is these largest structures with the highest shears, at the tails of the shear distribution, which dominate the magnification. These large shear-producing structures are rare, and so can be assumed to have a Poisson distribution. Hence the effect is to produce a shot-noise effect in the observed magnification power spectrum. Since the magnification is a non-linear function of the shear and convergence, this will not appear in the individual shear and convergence power spectra, but should be more apparent in their higher-order moments. Another consequence of this is that the cosmic variance, from realisation to realisation, should fluctuate quite wildly, which is the case here, and motivated the use of median statistics, rather than means which are more susceptible to this effect.

Since the magnification effect results from lensing from the largest structures and since the formation of structure evolves at different rates in different cosmologies, we would expect similar effects to be present in other cosmologies, but with differing degrees of severity. We have not studied the effect in other cosmologies but we might reasonably assume that the LCDM cosmology would display large effects because of the early development of structure.

We have shown that the effect can be damped by “clipping” the magnification field by removing the highest peaks. Removing the magnification values beyond 6σ in the distribution removes most of the effect, showing that indeed it is the highest peaks causing this effect. One may wonder if this is a purely numerical effect, as in the simulations there is a high sampling of lines of sight, including the high-magnification regions around clusters. In reality we may not expect to see such extreme effects as often since galaxy surveys only Poisson sample the magnification field. In addition, if the normalisation, σ_8 , were lower than our chosen value, the number of clusters would be expected to be smaller, again leading to fewer examples of extreme magnifications. However, even after clipping the magnification values beyond 6σ there is still a residual systematic. Only after clipping the values beyond 1σ in the distribution do we remove this effect significantly.

This all suggests that estimating the convergence power spectrum from magnification should be handled with care, unless evaluated at low redshifts. In addition, the estimation of higher-order statistics from the magnification will be equally affected by the shot-noise from individual, massive clusters which will also increase the effects of sampling variance on any large-scale measurement of the magnification field. Hence, while magnification remains a useful tool for probing the mass distributions in individual clusters, its value as a statistical probe over large scales may be complicated by these non-linear effects.

The results of Barber et al. (2000) for S_3 on large angular scales for different cosmological models, and the consis-

tent results of Jain et al. (2000) clearly show the strong Ω_m dependence of S_3 . Consequently, provided the convergence field is obtained by reconstruction from the shear, the S_3 statistic may be used to good effect to discriminate different cosmologies. In determining S_3 from their simulations, Jain et al. (2000) quote values for sources at redshift 1 only. It is reassuring to note that the magnitudes of their S_3 values on the different angular scales, determined in quite a different way from ours (by reconstruction of the convergence from the shear data), are in good agreement at the smallest scales where non-linear effects are expected to be most pronounced. As the angular scale increases our values fall slightly more rapidly with scale.

Our expression for the angular scale and redshift dependence for S_3 clearly demonstrates the necessity of knowing the redshift distribution of the sources. This is the same conclusion reached by Barber (2002) who reported the angular scale and redshift dependences for the shear variance.

However, now that the redshift dependence of S_3 is established for our LCDM cosmology ($S_3 \propto z_s^{-2.00}$), values determined from different surveys can be adjusted easily to a fixed median source redshift, enabling the combination and comparison of data from the different surveys. The only proviso here is that the redshift dependence of S_3 is likely to be cosmology dependent, since the magnitude of this statistic on a given angular scale and for a specific distribution of sources is known to be a discriminator of cosmologies. We have not yet investigated the redshift dependence of S_3 in other scenarios, although Barber et al. (2003) have reported on various aspects of S_3 from simulations and semi-analytical predictions in two different cosmologies. We would also hope to investigate the higher-order statistics for the convergence smoothed with a compensated filter in a later work, as this will allow more direct comparison with observed shear data.

The statistic $S_3\sigma_\kappa^2$ for a given angular scale is much less sensitive to the source redshift, as Bernardeau et al. (1997) also found for the Einstein-de Sitter cosmology. Figure 10 shows it to be approximately independent of redshift for high redshift sources and, using the results for the redshift dependence of the shear variance from Barber (2002) together with the redshift dependence of S_3 reported here, the statistic is shown to be only a very slowly increasing function of z_s for $z_s < 1$. Consequently, $S_3\sigma_\kappa^2$ may prove to be very useful for surveys in which the redshift distribution of the sources is uncertain.

6.2 Conclusions

For the convergence power spectrum, $\ell(\ell+1)C_\ell^{\kappa\kappa}/(2\pi)$, computed numerically from the lensing statistics in our simulations, we find excellent agreement with the values computed using a halo model. We can therefore have considerable confidence in our weak lensing statistics when applied to the shear, convergence, magnification and higher-order statistics. In addition, with this consistency, theoretical determinations of lensing statistics on a wider range of scales than can be achieved with numerical simulations may be used with increasing confidence.

Our results for one quarter the power in the magnification fluctuations, $\ell(\ell+1)C_\ell^{\delta\omega\delta\omega}/(8\pi)$, show that the magnification is susceptible to the effects of discrete massive clusters

and large variations across small angular intervals. These effects occur specifically beyond the weak lensing regime, and become apparent in the magnification even at low redshift and on small angular scales. Consequently, determination of the convergence field from magnification data should be treated with special attention.

Our simple mathematical description for $S_3(\theta, z_s)$, showing it to be closely proportional to z_s^{-2} for the LCDM cosmology, makes it particularly simple to compare and combine the results from different surveys in which the median redshifts of the galaxies may be different.

Finally, we found directly, and through combination with the mathematical expressions for the shear variance and S_3 , that the combined statistic $S_3\sigma_\kappa^2$ is only a very slowly increasing function of redshift for low redshift sources and approximately independent of redshift at high redshift, as has been found in the Einstein-de Sitter cosmology. This statistic, therefore, may be useful in comparing and combining the data from different surveys with different galaxy redshift distributions.

ACKNOWLEDGEMENTS

This work has been supported by PPARC and carried out with facilities provided by the University of Sussex and the University of Edinburgh. AJB was supported in part by the Leverhulme Trust. ANT is a PPARC Advanced Fellow, and thanks the University of Sussex for its hospitality, where this work began. The original code for the three-dimensional shear computations was written by Hugh Couchman of McMaster University. There were many useful discussions with Ludo Van Waerbeke, Henk Hoekstra, Peter Schneider, Antonio da Silva, Rachel Webster, Andrew Liddle, Andrew Melatos, Chris Fluke, Martin White, Chris Vale and David Bacon.

REFERENCES

- Bacon D. J., Massey R., Refregier A. R., Ellis R. S., 2002, astro-ph/0203134 (submitted MNRAS)
- Bacon D. J., Refregier A. R., Ellis R. S., 2000, MNRAS, 318, 625
- Bacon D. J., Taylor A. N., 2002, astro-ph/0212266 (submitted MNRAS)
- Barber A. J., 2002, MNRAS, 335, 909
- Barber A. J., Munshi D., Valageas P., 2003, astro-ph/0304451 (submitted MNRAS)
- Barber A. J., Thomas P. A., Couchman H. M. P., 1999, MNRAS, 310, 453
- The figure shows the comparisons assuming sources at redshifts 0.5, 1.0 and 2.0.
- Barber A. J., Thomas P. A., Couchman H. M. P., Fluke C. J., 2000, MNRAS, 319, 267
- Bartelmann M., Narayan R., 1995, Ap. J., 451, 60
- Bartelmann M., Schneider P., 2001, Physics Reports, 340, 291
- Bernardeau F., Van Waerbeke L., Mellier Y., A&A, 1997, 322, 1
- Blandford R. D., Saust A. B., Brainerd T. G., Villumsen J. V., 1991, MNRAS, 251, 600
- Broadhurst T. J., Taylor A. N., Peacock J. A., 1995, Ap. J., 438, 49
- Brown M. L., Taylor A. N., Hambly N. C., Dye S., 2002a, MNRAS, 333, 501
- Brown M. L., Taylor A. N., Bacon D. J., Gray M. E., Dye S., Meisenheimer K., Wolf C., 2002b, astro-ph/0210213

- Catelan P., Kamionkowski M., Blandford R. D., 2001, MNRAS, 323, 713
- Couchman H. M. P., Barber A. J., Thomas P. A., 1999, MNRAS, 308, 180
- Couchman H. M. P., Thomas, P. A., Pearce F. R., 1995, Ap. J., 452, 797
- Crittenden R., Natarajan P., Pen U., Theuns, T., 2001, ApJ, 545, 561
- Croft. R. A. C., Metzler C. A., 2001, ApJ, 545, 561
- Dye S., Taylor A.N., Thommes E.M., Meisenheimer K., Wolf C., Peacock J.A., 2001, MNRAS, 321, 685
- Hamilton A. J. S., Matthews A., Kumar P., Lu E., 1991, Ap. J., 374, L1
- Heavens A. F., Refregier A., Heymans C., 2000, MNRAS, 319, 649
- Heymans C., Heavens A. F., 2002, astro-ph 0208220 (submitted MNRAS)
- Hoekstra H., Yee H. K. C., Gladders M. D., 2002, ApJ, 577, 595
- Hoekstra H., Yee H. K. C., Gladders M. D., Barrientos L. F., Hall P. B., Infante L., 2002, ApJ, 572, 55
- Jain B., Seljak U., 1997, Ap. J., 484, 560
- Jain B., Seljak U., White S., 2000, Ap. J., 530, 547
- Jain B., 2002, ApJLett, 580, L3
- Jarvis M., Bernstein G., Jain B., Fischer P., Smith D., Tyson J. A., Wittman D., 2002, astro-ph/0210604
- Kaiser N., 1995, Ap. J., 439, L1
- Kaiser N., Squires G., 1993, Ap. J., 404, 441
- Kaiser N., Wilson G., Luppino G. A., 2000, astro-ph/0003338
- King L., Schneider P., 2002, astro-ph 0208256 (submitted A&A)
- Mackey J., White M., Kamionkowski M., 2002, MNRAS, 332, 788
- Maoli R., Van Waerbeke L., Mellier Y., Schneider P., Jain B., Bernardeau F., Erben T., Fort B., 2001, A&A, 368, 766
- Mellier Y., Van Waerbeke L., Maoli R., Schneider P., Jain B., Bernardeau F., Erben T., Fort B., 2001, astro-ph/0101130
- Moessner R., Jain B., 1998, MNRAS, 294, L18
- Peacock J. A., Dodds S. J., 1996, MNRAS, 280, L19
- Peacock J. A., Smith R. E., 2000, MNRAS, 318, 1144
- Peebles P. J. E., 1980, "The large-scale structure of the universe, Princeton University Press, Princeton, NJ
- Pen U., Lee J., Seljak U., 2000, ApJ, 543, L107
- Pen U., Van Waerbeke L., Mellier Y., 2002, ApJ, 567, 31
- Rhodes J., Refregier A., Groth E. J., 2001, Ap. J., 552, 85
- Schneider P., Ehlers J., Falco E. E., 1992, 'Gravitational Lenses,' Springer-Verlag, ISBN 0-387-97070-3
- Seitz S., Schneider P., 1996, A&A, 305, 383
- Seljak U., 2000, MNRAS, 318, 203
- Smith R. E., Peacock J. A., Jenkins A., White S. D. M., Frenk C. S., Pearce F. R., Thomas P. A., Efstathiou G., Couchman H. M. P., 2002, astro-ph/0207664
- Taylor A.N., 2001, astro-ph/0111605 (submitted Phys Rev Lett)
- Valageas P., Barber A. J., Munshi D., 2003, astro-ph/0303472 (submitted MNRAS)
- Van Waerbeke L., Bernardeau F., Mellier, Y., 1999, A&A, 342, 15
- Van Waerbeke L., Mellier Y., Erben T., Cuillandre J. C., Bernardeau F., Maoli R., Bertin E., McCracken H. J., Le Fèvre O., Fort B., Dantel-Fort M., Jain B., Schneider P., 2000a, A&A, 358, 30
- Van Waerbeke L., Mellier Y., Erben T., Cuillandre J. C., Bernardeau F., Maoli R., Bertin E., McCracken H. J., Le Fèvre O., Fort B., Dantel-Fort M., Jain B., Schneider P., 2000b, astro-ph/0008178
- Van Waerbeke L., Mellier Y., Radovich M., Bertin E., Dantel-Fort M., McCracken H. J., Le Fèvre O., Foucaud S., Cuillandre J. C., Erben T., Jain B., Schneider P., Bernardeau F., Fort B., 2001, A&A, 374, 757
- Wittman D. M., Tyson J. A., Kirkman D., Dell'Antonio I., Bernstein G., 2000, Nature, 405, 143